J. Micromech. Microeng. **7** (1997) 14–23. Printed in the UK PII: S0960-1317(97)78160-9

Porous silicon as the carrier matrix in microstructured enzyme reactors yielding high enzyme activities

J Drott†§, K Lindström†, L Rosengren‡ and T Laurell†

† Department of Electrical Measurements, Lund Institute of Technology, Lund University, PO Box 118, S-221 00 Sweden
‡Division of Electronics, Department of Technology, Uppsala University, PO Box 534, S-751 21 Uppsala, Sweden

Received 23 September 1996, accepted for publication 3 December 1996

Abstract. Miniaturization and silicon integration of micro enzyme reactors for applications in micro total analysis systems (μTASs) require new methods to achieve structures with a large surface area onto which the enzyme can be coupled. This paper describes a method to accomplish a highly efficient silicon microstructured enzyme reactor utilizing porous silicon as the carrier matrix. The enzyme activity of microreactors with a porous layer was recorded and compared with a microreactor without the porous layer.

The microreactors were fabricated as flow-through cells comprising 32 channels, 50 μm wide, spaced 50 μm apart and 250 μm deep micromachined in $\langle 110 \rangle$ oriented silicon, p type (20–70 Ω cm), by anisotropic wet etching. The overall dimension of the microreactors was 13.1 $\times$ 3.15 mm. To make the porous silicon layer, the reactor structures were anodized in a solution of hydrofluoric acid and ethanol. In order to evaluate the surface enlarging effect of different pore morphologies, the anodization was performed at three different current densities, 10, 50 and 100 mA cm^{-2}.

Glucose oxidase was immobilized onto the three porous microreactors and a non-porous reference reactor. The enzyme activity of the reactors was monitored following a colorimetric assay.

To evaluate the glucose monitoring capabilities, the reactor anodized at 50 mA cm^{-2} was connected to an FIA system for glucose monitoring. The system displayed a linear response of glucose up to 15 mM using an injection volume of 0.5 μl.

The result from the studies of glucose turn-over rate clearly demonstrates the potential of porous silicon as a surface enlarging matrix for micro enzyme reactors. An increase in enzyme activity by a factor of 100, compared to the non-porous reference, was achieved for the reactor anodized at 50 mA cm^{-2}.

1. Introduction

In the development of micro total analysis systems, μTASs, new components and concepts are reported frequently [1, 2]. An overall trend in this progress is towards materials more dedicated to the application, such as in [3] and [4]. Today, microsensors for low-molecular-weight compounds, such as pO_2, pH and pCO_2, are commonly integrated in these microsystems [5]. However, for the recording of more complex compounds, e.g. glucose, lactate, glutamate or acetylcholine, enzymatic detection is a prerequisite. For long-term stability and continuous monitoring of biomolecules the use of enzyme reactors in a flow-through system has become a standard technique.

A key issue in the design of enzyme reactors is the surface enlarging properties of the carrier matrix in the reactor. This becomes even more pronounced when enzyme reactors are being miniaturized and integrated with other μTAS components. Our earlier work on microreactors has utilized anisotropic wet etching of $\langle 110 \rangle$ oriented silicon to micromachine a surface enlarging structure comprising channels with vertical walls [6]. Other groups have investigated microreactor designs having either a long single v-groove [7] or several parallel v-grooves [8]. The most efficient design of these micro enzyme reactors, in terms of achieved reactor area versus occupied wafer area, is the parallel trench structure comprising vertical trenches. However, all these microreactors still suffer from lack of long-term stability due to the relatively low surface area of the coupling matrix: planar silicon surfaces. A porous surface of the flow channels would increase the surface area for enzyme coupling.

Porous silicon as a material for chemical sensor

§ Internet: johan.drott@elmat.lth.se

0960-1317/97/010014+10$19.50

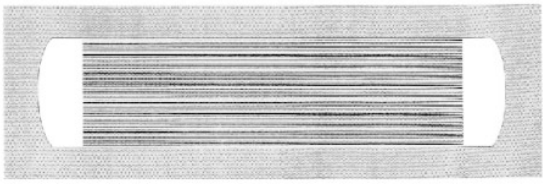

Figure 1. The reactor design having 32 trenches; 50 μm wide and spaced 50 μm apart. The length of the trenches was 11 mm on the original mask. The overall dimensions of the reactors on the mask were 13.1 mm $\times$ 3.15 mm.

applications has previously been reported [9], where a porous silicon frit provides the electrochemical bridge contact for the reference electrode. Work utilizing porous silicon as a biosensor substrate material has also been reported [10]. Our group has recently reported the application of porous silicon as a carrier matrix for immobilized enzymes [11], and also demonstrated its potential use in micro enzyme reactors.

To accomplish the long-sought goal of continuous glucose measurements, utilizing a biosensor based on enzymatic detection with micro enzyme reactors, several problems must be surmounted. A most important issue is to be able to couple such large amounts of enzyme to the microreactor that long-term viability is accomplished. Our previously reported reactor designs [6] have shown that efforts in increasing the surface area available for enzyme coupling in the microreactor yield a proportional increase in enzyme activity. However, for long-term stability of the monitoring, new methods to further increase the surface area of the microreactors must be investigated.

This paper reports porous silicon on a structure of several parallel vertical channels resulting in a superior increase (100 times) in enzyme activity when compared to an identical microreactor without the porous silicon layer. The concept is novel and the results clearly demonstrate the potential of porous silicon as a coupling matrix in silicon micro enzyme reactors.

2. Materials and methods

2.1. Reactor fabrication

The design of the microreactor comprised two basins for the flow inlet and outlet interconnected via an 11 mm long trench structure having 32 channels; 50 μm wide and spaced 50 μm apart (figure 1). The total occupied wafer area of the reactor was 41.3 mm^2 (3.15 mm $\times$ 13.1 mm).

For the fabrication 380 μm thick $\langle 110 \rangle$ oriented silicon wafers were used. The wafers were of p type with a resistivity of 20–70 Ω cm. To make good p^+ back contact, for the subsequent electrochemical anodization procedure, the back sides of the wafers were ion implanted with boron (100 keV, 5 $\times$ 1015 atoms cm^{-2}). After the implantation, a 1.1 μm thick mask oxide was thermally grown in wet oxygen, at a temperature of 1050 °C. This step consumed 0.5 μm of the ion implanted silicon. However, the remaining doping of the underlying silicon sufficed for a good electric contact.

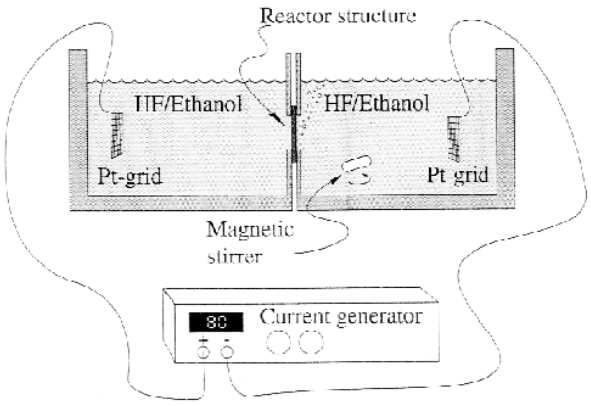

Figure 2. The in-house designed anodization cell.

Standard lithography methods were applied to pattern the silicon dioxide masking layer. The structures were etched in KOH (70 g/100 ml H_2O) for 2 h at 80 °C. Ultrasonic agitation (Sonorex Super Digital 10 P, Bandelin, Germany) was used during the anisotropic etching. After the etching, the silicon dioxide etch mask was removed in HF.

2.2. Porous silicon fabrication

A porous silicon layer on the front side (channel side) of each microreactor structure was achieved by anodizing the structures in a solution containing HF (48%) and ethanol (96%), mixing ratio (1:1). For the anodization an in-house fabricated sample holder was used (figure 2). The anodization was performed at constant current densities of 10, 50 or 100 mA cm^{-2}. A magnetic stirrer in the HF solution removed gas bubbles from the reactor surface.

After anodization the porous microreactors obtained were thoroughly rinsed in H_2O and stored for several days in H_2O at 8 °C, prior to the enzyme coupling.

2.3. Enzyme coupling

Glucose oxidase was coupled to the porous microreactor surfaces, following a standard procedure for immobilizing enzyme to silica [6]. As a reference, a microreactor without a porous layer was also subjected to the enzyme immobilization procedure. The enzyme was immobilized on the non-porous and the three porous microreactors simultaneously. The immobilization was performed in beaker solutions, thus enzyme was coupled to the entire chip. After the immobilization the microreactors were stored in phosphate buffer solution, PBS (pH 7), at 8 °C.

2.4. Enzyme activity monitoring—steady state

The enzyme activity of the micro enzyme reactors was monitored following a colorimetric assay, previously reported in [6]. To achieve a flow-through cell where only the enzyme activity of the surface within the reactor was monitored, the reactor under evaluation was mounted in an in-house designed fixture (figure 3(a)) fabricated in Perspex.

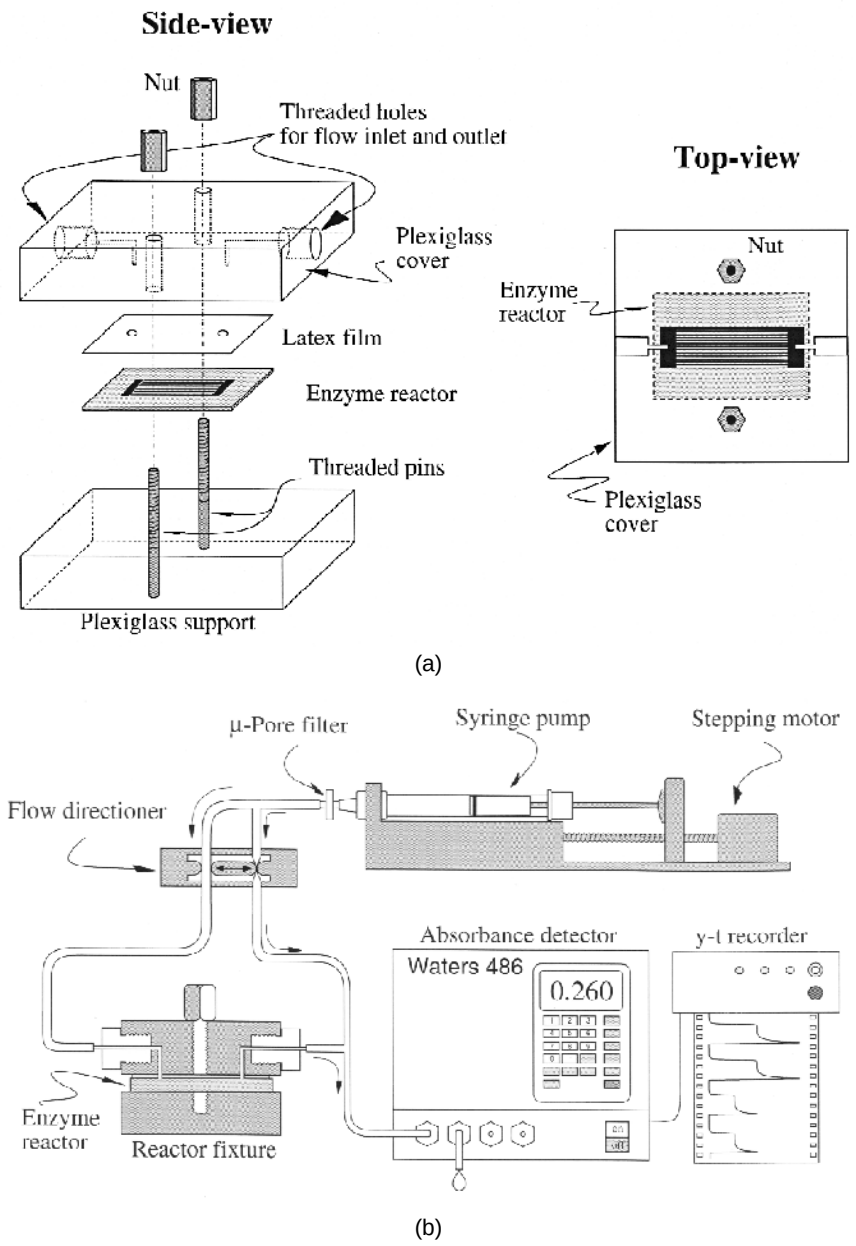

Figure 3. (a) The Perspex fixture for the micro enzyme reactor. (b) The system set-up for the enzyme activity determination.

As a seal between the top surface of the reactor and the Perspex lid, a sheet of latex was used (figure 3(a)). A colorimetric hydrogen peroxide reagent, i.e. Trinder reagent [12], containing peroxidase and glucose, was pumped through the reactors (figure 3(b)). The resulting colour shift due to the conversion of hydrogen peroxide, produced by the GOD catalysed glucose turn-over, was monitored by a Waters 486 tunable absorbance detector (Millipore, Millford, MA, USA). The reactors were exposed to glucose concentrations from 0.1 to 5 mM. The measurements were performed for each glucose concentration at increasing flow rates until enzyme kinetic conditions prevailed. The enzyme activity of the different reactors was calculated from the monitored absorbance shift [6].

2.5. Glucose measurements—flow injection mode with O_2 recording

In order to study a porous micro enzyme reactor in a measuring situation the microreactor anodized at 50 mA cm^{-2} was connected to an FIA system (figure 4). The reactor was perfused with PBS and samples containing glucose in PBS were injected into the flow using an electrically controlled injection valve, C24Z (VICI, Valco Instruments, Houston, TX, USA). The injection volume used was 0.5 μl. The conversion of glucose was recorded by monitoring the oxygen consumption with an in-house fabricated Clark type electrode, previously described in [13]. The electrode current was recorded with a Keithley 428 current amplifier (Keithley, Cleveland, OH, USA). To set the flow rate, 25 μl min^{-1}, of the mobile phase (PBS)

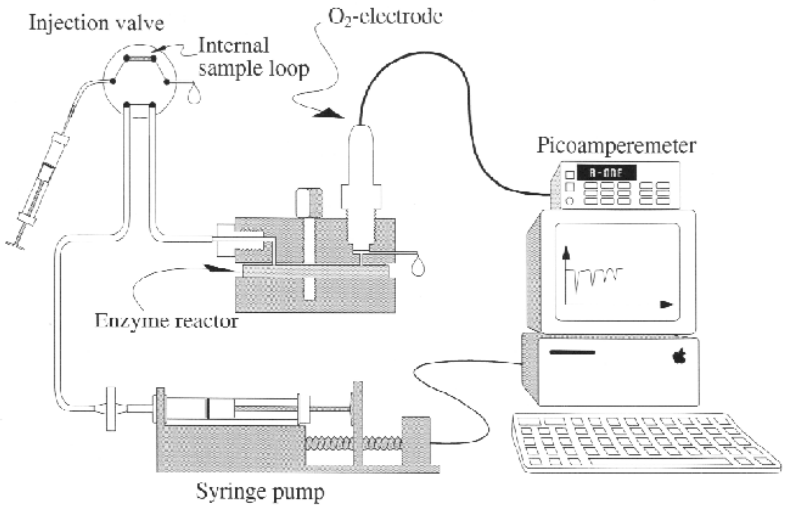

Figure 4. The flow injection set-up.

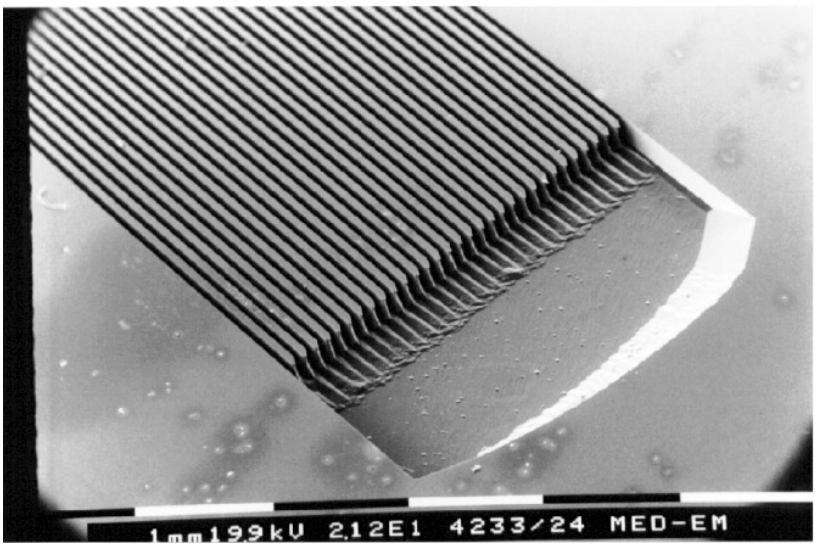

Figure 5. An SEM view of a microreactor without the porous layer. Note the loss in trench length at the beginning of the trenches.

an in-house built syringe pump (stepping motor controlled) was used. The whole system was computer controlled using LabVIEW software from National Instruments, Austin, TX, USA.

3. Experiments and results

3.1. Reactor fabrication

Anisotropic wet etching to achieve a trench structure with several parallel trenches, using the vertical {111} etch stop planes in (110) silicon, inherently results in a loss of trench length due to the exposed convex corners at the wall endings. This reduced the achieved length of the trenches compared to the original design of the microreactor, in this case a total loss of trench length of 1 mm/trench was noted. Thus, the resulting geometry of the microreactor was a 10 mm long parallel trench structure comprising 32 trenches, 50 μm wide and 250 μm deep (figure 5). The reactor dead volume was 6.3 μl.

The total surface area in the microreactor available for enzyme coupling, including the two basins at each end of the trench structure and the surface of the channels (walls and bottoms), was 189.5 mm^2. The gain in surface area available for enzyme coupling can be expressed in terms of a normalized reactor area (NRA).

$$\mathrm{NRA} = \frac{\text{total reactor surface area}}{\text{occupied wafer area}}.$$

The fabricated trench type microreactor had an NRA factor of 4.6, since the totally occupied wafer area of each reactor was 41.3 mm^2.

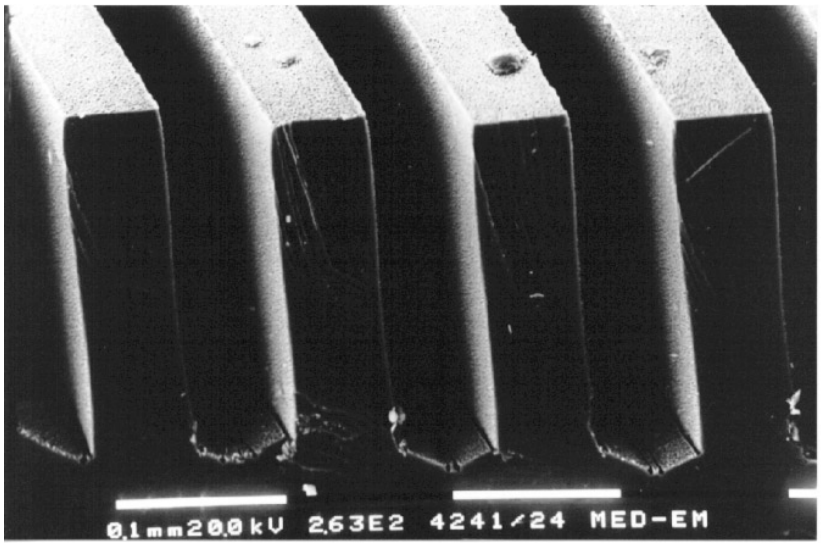

(a)

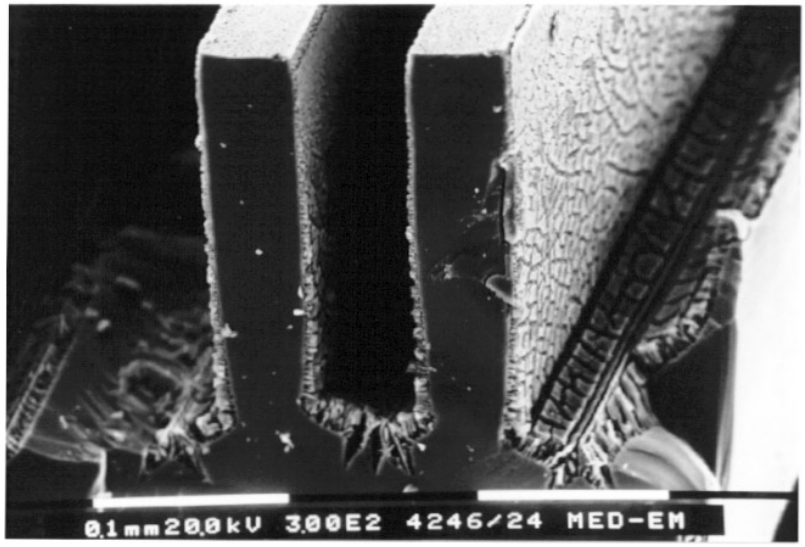

(b)

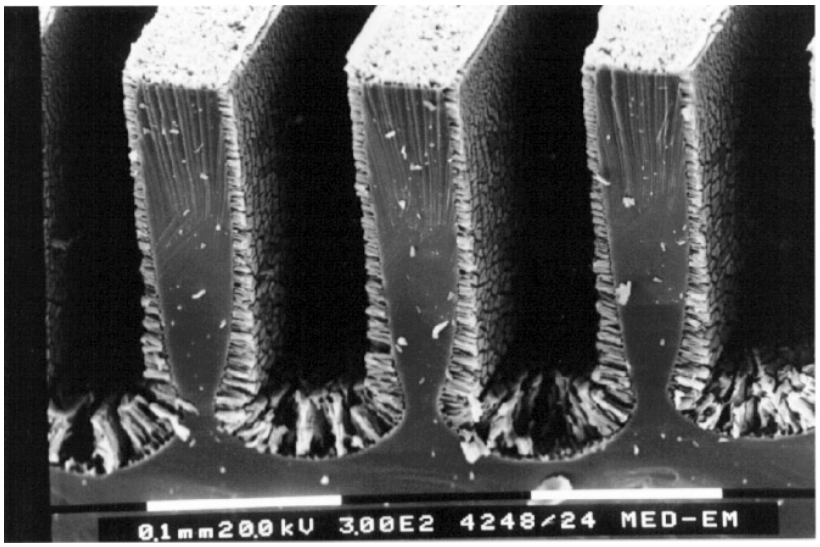

(c)

Figure 6. SEM view cross sections of the three porous reactors, anodized at (a) 10 mA cm^{-2} (10 min), (b) 50 mA cm^{-2} (5 min) and (c) 100 mA cm^{-2} (5 min).

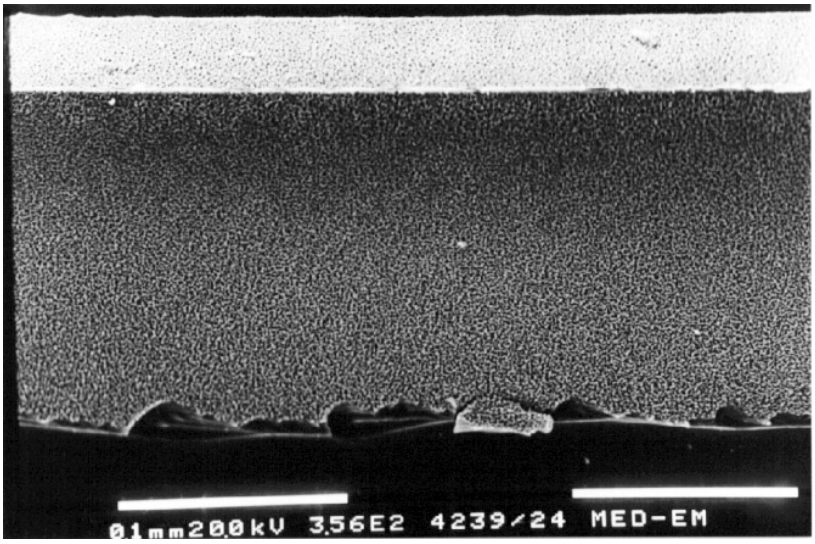

(a)

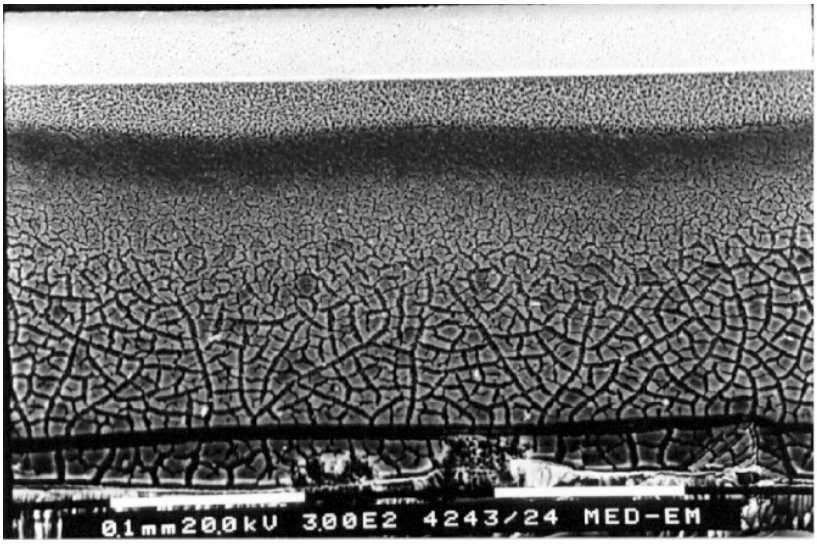

(b)

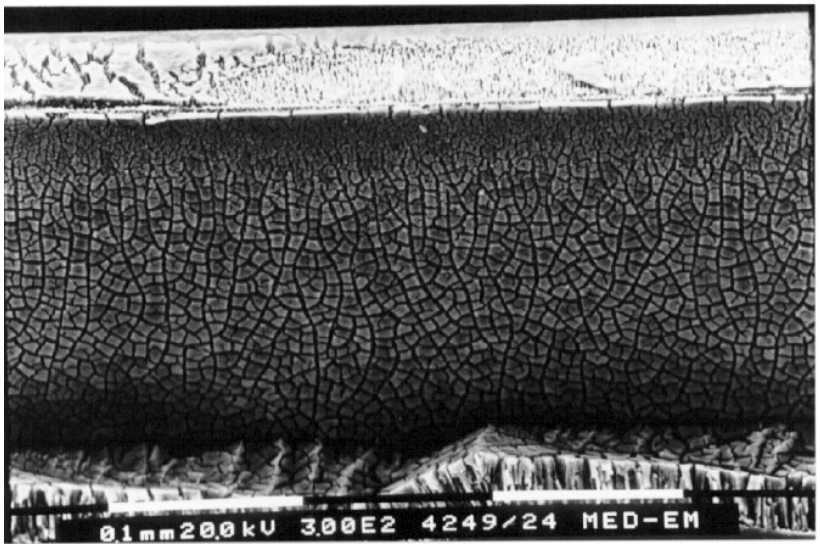

(c)

Figure 7. Side views of the porous channel walls: (a) 10 mA cm^{-2}; (b) 50 mA cm^{-2}; (c) 100 mA cm^{-2}.

3.2. Porous silicon fabrication

Porous silicon of three different morphologies was obtained on the microreactors by anodizing the reactor structures at 10, 50 or 100 mA cm^{-2}. The 10 mA cm^{-2} reactor was anodized for 10 min and the 50 and 100 mA cm^{-2} reactors were anodized for 5 min. The difference in anodization time was to compensate to some extent for the increasing pore propagation rate at higher current densities. In spite of the shortened anodization time, the enzyme reactors anodized at higher current densities displayed a much thicker porous layer, as can be seen in the cross-section SEM views in figure 6.

The average depth of the porous layer on the standing trench walls (table 1) was estimated from figure 6.

The surface morphologies achieved at different current densities are revealed in figure 7. The 'dried lake' texture of the trench wall surface is particularly pronounced at increasing current density and at the lower part of the walls. Higher current density favours the formation of larger pores [14] which results in the 'dried lake' texture. This can also be an explanation of the larger pores at the bottom of the trenches, since the current density increases at these locations due to the sharp edges. At these locations minority charge carriers (holes), which are essential for the pore formation process, are attracted [15] and larger pores are formed.

3.3. Enzyme activity monitoring

The enzyme activity of the non-porous reference and the porous enzyme reactors was recorded by perfusing the reactor with glucose in Trinder reagent. A measurement of the colour shift, recorded by the absorbance detector, was achieved by switching the flow path to either perfuse the reactor or bypass it (figure 3(b)). The enzyme activity is calculated from the recorded absorbance shift, Δ Abs.

The absorbance response was recorded for the microreactors at increasing flow rates. By increasing the flow rate the subversion of glucose reached the conditions where the reaction was limited by the enzyme kinetics, and thus not substrate diffusion limited. A typical absorbance recording of 0.5 mM glucose for the microreactor anodized at 50 mA cm^{-2} is presented in figure 8. The sharp peak appearing each time the reagent was passed through the reactor was due to the progress of the enzymatic reaction in the stagnant reactor volume during bypass.

The enzyme activity and thus the glucose turn-over rate (the number of catalysed glucose molecules per time unit) was calculated from the absorbance shift and the molar absorption coefficient of the colour compound [6]. The turn-over rate versus flow rate recorded at 0.5 mM glucose for the microreactors is presented in figure 9.

The enzyme activity of the microreactors was calculated from absorbance measurements performed at 0.1, 0.5, 1, 2 and 5 mM glucose. The enzyme activity at each glucose concentration was estimated at the maximum flow rate employed, which ensured that enzyme kinetics prevailed. The recorded turn-over rate versus the glucose concentration for the three porous micro enzyme reactors is presented in figure 10.

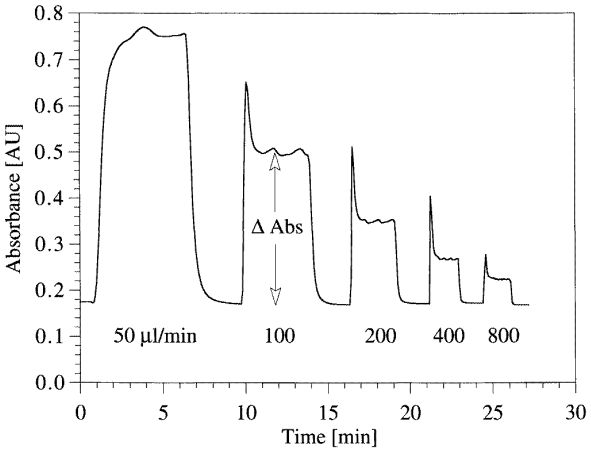

Figure 8. The absorbance at 0.5 mM glucose for the 50 mA cm^{-2} reactor recorded at increasing flow rates.

From figure 10 it is evident that the maximum turn-over rate (V_{max}) was not reached for any of the porous microreactors since it was impossible to apply high enough flow rates to the system at higher glucose concentrations.

To be able to evaluate the surface enlarging effect of the porous layer, although V_{max} was not reached, the highest recorded turn-over rate ($\hat{V}$) was used to estimate the enzyme activity amplification of the porous reactors as compared to the non-porous reference reactor. The amplification factor of the enzyme activity was calculated for the different microreactors for three glucose concentrations, 1, 2 and 5 mM (table 2).

3.4. Glucose measurements—flow injection mode with O_2 recording

Measurements were performed on samples of glucose (0.5–25 mM) using a 0.5 μl injection volume. Three samples of each glucose concentration were injected with an interval of 240 s in the mobile phase, PBS (pH 7), at a flow rate of 25 μl min^{-1}. A flow injection sequence (0.5–9 mM) recorded by a Clark electrode is seen in figure 11.

The peak area average at each glucose concentration (0.5–25 mM) is seen in the calibration plot in figure 12.

4. Discussion

The achieved results demonstrate the potential in combining porous silicon and standard methods of microstructuring to achieve highly efficient micro enzyme reactors. As indicated in the cross section SEM views (figure 6), the current density during the anodization determines the thickness of the porous layer. Also, at higher current density a more pronounced piping of pores perpendicular to the surface is noted. For the reactors anodized at higher current density, the surface of the trench walls displays a 'dried lake' texture (figure 7). In the case of the 50 mA cm^{-2} reactor the 'dried lake' texture was only visible at the lower part of the trench walls. This is due to the process of pore formation, earlier demonstrated by

Table 1. The depth of the porous layer.

	Current density		
	10 mA cm^{-2}	50 mA cm^{-2}	100 mA cm^{-2}
Anodization time (min)	10	5	5
Porous depth (μm)	1	7	12

Table 2. The amplification of the enzyme activity for the three porous microreactors versus the non-porous reference reactor.

	Enzyme activity amplification		
Glucose conc. (mM)	10 mA cm^{-2}	50 mA cm^{-2}	100 mA cm^{-2}
1.0	48	85	56
2.0	57	116	70
5.0	51	95	41
Mean$\pm$std.	52 ± 5	99 ± 16	56 ± 15

Table 3. The IF factor for different reactor designs. It should be noted that for the non-porous reference the highest recorded turn-over rate ($\hat{V}$) was used as V_{max}.

Structure	Total reactor area (mm^2)	V_{max} (nmol min^{-1})	IF (nmol min^{-1} mm^{-2})
20 μm reactor [6]	515.0	33.0	6.4×10^{-2}
Non-porous reference [11]	47.8	0.4	8.4×10^{-3}
Non-porous reference[a]	189.5	0.7	3.7×10^{-3}

[a] Reference reactor in this work.

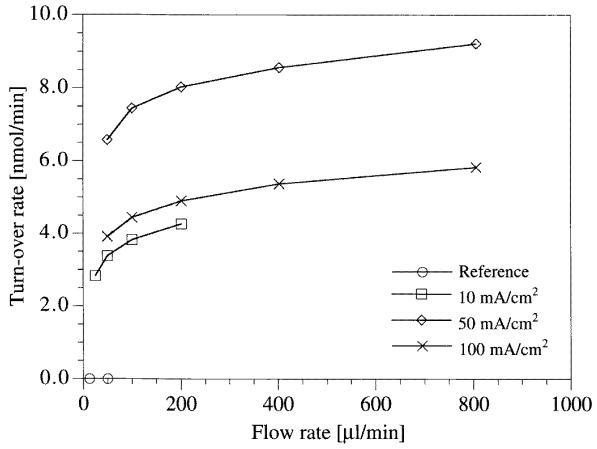

Figure 9. The enzyme activity at 0.5 mM glucose measured at different flow rates for the micro enzyme reactors.

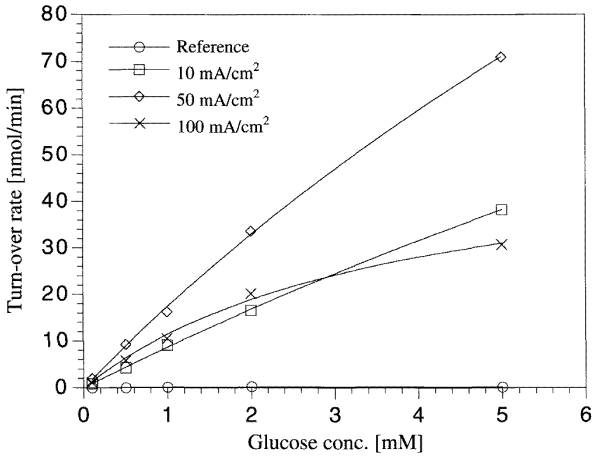

Figure 10. Recorded enzyme activity versus glucose concentration for the microreactors.

Smith and Collins [14]. At the bottom of the trenches the sharp edges focus the electrostatic field, which attracts the minority charge carriers. This in turn increases the current density at the trench bottom which gives rise to the formation of larger pores. The surface properties of the coupling matrix can be tailored by proper control of the electrochemical process during the porous silicon formation.

As can be seen in the amplification table (table 2), a maximum increase in enzyme activity of a factor of approximately 100 was recorded, for the microreactor anodized at 50 mA cm^{-2}, compared to the non-porous reference reactor. This indicates that the pore size achieved at 50 mA cm^{-2} was most favourable although the 10 mA cm^{-2} reactor provides a higher surface enlargement with its finer pore structure, which implies that not only the pore size is determining the matrix property.

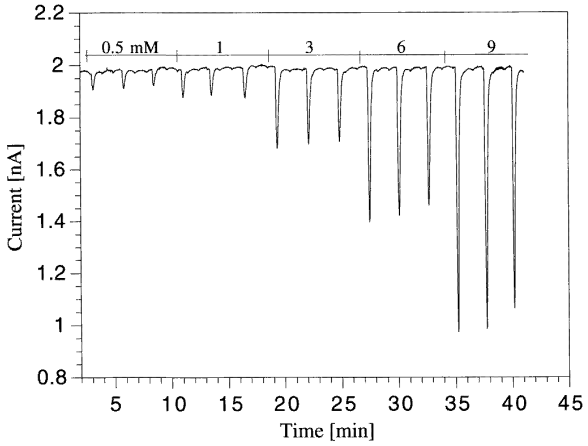

Figure 11. Glucose (0.5–9 mM) measured by the FIA system with the 50 mA cm^{-2} reactor.

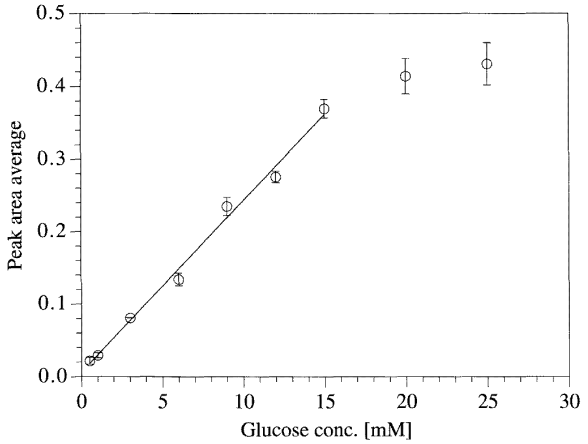

Figure 12. The calibration plot for glucose using FIA and the 50 mA cm^{-2} reactor.

The difference in enzyme activity between the three porous enzyme reactors is defined by the depth of the porous regions and by the average pore size. A significant difference in porous depth between the microreactor anodized at 10 mA cm^{-2} and the microreactors anodized at higher current densities was noted (table 1). This difference in pore depth is a possible explanation for the lower enzyme activity recorded for the 10 mA cm^{-2} reactor, compared to the reactor anodized at 50 mA cm^{-2}. The porous layer was shallower for the 50 mA cm^{-2} reactor, compared to the 100 mA cm^{-2} reactor, yet the 50 mA cm^{-2}-reactor displayed a significantly higher enzyme activity. Thus, the difference in activity between the 50 mA cm^{-2} and the 100 mA cm^{-2} reactors in this case must be determined by the pore size and the surface enlargement of the porous layer.

To describe how efficiently the wafer area has been utilized for the micro enzyme reactor and to be able to compare it to other micro enzyme reactors the efficiency factor (EF) can be used. EF is determined by

$$\mathrm{EF} = \frac{\hat{V}}{\text{occupied wafer area}} \left(\frac{\text{nmol}}{\text{min mm}^2} \right)$$

where $\hat{V}$ is the highest recorded enzyme activity (nmol min^{-1}). In the case of the microreactor anodized at 50 mA cm^{-2} the corresponding EF was 1.8 nmol min^{-1} mm^{-2}. Compared to the non-porous reference micro enzyme reactor an increase in EF by a factor of 100 was achieved.

Our work on micro enzyme reactors has been focused on increasing the efficiency of the carrier matrix. Therefore, the yield of the immobilization procedure from one batch to another must be accounted for. To be able to evaluate the immobilization procedure, an immobilization factor, IF, is defined as

$$\mathrm{IF} = \frac{\hat{V}}{\text{total reactor area}} \left(\frac{\text{nmol}}{\text{min mm}^2} \right).$$

Earlier work on silicon integrated parallel trench enzyme reactors and planar silicon surfaces [6] has studied the enzyme activity of non-porous reactors with channel widths of 20 μm, denoted the 20 μm reactor, and a planar silicon surface was used in [11] as a reference. The performance of these reactors with respect to $\hat{V}$ and IF is compared with the reference reactor investigated in this paper (table 3). The difference in IF between the different reactors in table 3 was due to ageing of the enzyme batch. All reactors in table 3 were immobilized with enzyme from the same lot and the work was done over a period of 3 years.

The IF can be used to compensate for the ageing of the enzyme between the different micro enzyme reactor generations. The earlier experiments on the 20 μm reactor have an IF that is 17 times higher than in the recent studies, on porous silicon microreactors. In case of the 50 mA cm^{-2} reactor an EF of 31 nmol min^{-1} mm^{-2} could thus be expected (1.8 nmol min^{-1} mm^{-2} recorded). When compared to the best previous reported reactor, the 20 μm reactor [6], having an EF of 0.7 nmol min^{-1} mm^{-2}, the reactor anodized at 50 mA cm^{-2} can be expected to display an increase in EF of 44-fold when fresh enzymes are used.

The FIA system (figure 4), displayed a linear glucose response to 15 mM, using the 50 mA cm^{-2} reactor (figure 11). At higher glucose concentrations the subversion of glucose was restricted by oxygen depletion. If a longer linear response range is desired a smaller injection volume is required, which due to the system dispersion inherently will dilute the sample.

In the perspective of μTAS comprising enzyme reactors as a versatile tool for biomolecule monitoring, a major problem has been the low surface area available. Attempts to overcome this have been presented by introducing flow-through columns that are packed with microbeads serving as the carrier matrix [16]. The introduction of porous silicon in silicon integrated enzyme reactors avoids all problems encountered with the microbead handling and the packing of the columns. Furthermore, porous silicon is process compatible with other microstructuring techniques which to a great extent facilitates the integration of porous silicon reactors in a μTAS.

5. Conclusions

Our previous studies of porous silicon have shown that it is a material well suited as a coupling matrix for enzymes. For creating highly efficient micro enzyme reactors porous silicon combined with standard methods of microstructuring silicon is a most promising method. This paper shows that porous silicon can be fabricated on high-aspect-ratio silicon enzyme reactors. An ongoing and more thorough study on the effect of pore depth and pore size will yield further optimized porous layers and thus silicon integrated micro enzyme reactors with improved performance.

Acknowledgments

The authors would like to thank Kungliga Fysiografiska Sällskapet i Lund, Lund Institute of Technology (LTH) and Carl Tryggers Stiftelse for their financial support.

References

[1] Manz A, Harrison D J, Verpoorte E and Weidmer H M 1993 Planar chips technology for miniturization of separation systems: a developing perspective in chemical monitoring *Advances in Chromatography* vol 33, ed P R Brown and E Grushka pp 1–66

[2] van der Schoot B H, Jeanneret S, van der Berg A and de Rooij N F 1993 Microsystems for flow injection analysis *Anal. Methods Instrum.* **1** 38–42

[3] Dietrich T R, Abraham M, Diebel J, Lacher M and Ruf A 1993 Photoetchable glass for microsystems: tips for atomic force microscopy *J. Micromech. Microeng.* **3** 187–9

[4] Arquint Ph 1994 Integrated blood gas sensor for pO_2, pCO_2 and pH based on silicon technology *PhD Thesis* pp 173–93

[5] Arquint Ph 1993 Integrated blood gas sensor for pO_2, pCO_2 and pH *Sensors Actuators* B **13/14** 340–4

[6] Laurell T, Rosengren L and Drott J 1995 Silicon integrated enzyme reactors *Biosensors Bioelectron.* **10** 289–99

[7] Suda M, Sakuhara T, Murakami Y and Karube I 1993 Micromachined detectors for an enzyme-based FIA *Appl. Biochem. Biotechnol.* **10** 11–5

[8] Xie B, Danielsson B, Norberg P, Winquist F and Lundström I 1992 Development of a thermal micro-biosensor fabricated on a silicon chip *Sensors Actuators* B **6** 127–30

[9] Smith R L and Scott D C 1986 An integrated sensor for electrochemical measurements *IEEE Trans. Biomed. Eng.* **BME-33** 83–90

[10] Thust M, Schöning M J, Frohnhoff S, Arens-Fischer R, Kordos P and Lüth H 1996 Porous silicon as a substrate material for potentiometric biosensors *Meas. Sci. Technol.* **7** 26–9

[11] Laurell T, Drott J, Rosengren L and Lindström K 1996 Enhanced enzyme activity in silicon integrated enzyme reactor utilizing porous silicon as carrier matrix *Sensors Actuators* B **31** 161–6

[12] von Gallati H 1997 Aktivitätsbestämmung von Peroxidase mit Hilfe des Trinder-Reagens *J. Clin. Chem. Biochem.* **15** 699–703

[13] Laurell T 1992 A continuous glucose monitoring system based on microdialysis *J. Med. Eng. Technol.* **16** 187–93

[14] Smith R L and Collins S D 1992 Porous silicon formation mechanisms *J. Appl. Phys.* **71** R1–R22

[15] Lehmann V 1990 Formation mechanism and properties of electrochemically etched trenches in n-type silicon *J. Electrochem. Soc.* **173** 653–9

[16] Xie B, Danielsson B, Norberg P, Winquist F and Lundström I 1993 Miniaturised thermal biosensors *Sensors Actuators* B **15/16** 443–7